Biochimica et Biophysica Acta 1788 (2009) 522–531

Contents lists available at ScienceDirect

Biochimica et Biophysica Acta

journal homepage: www.elsevier.com/locate/bbamem

Sensory rhodopsin II/transducer complex formation in detergent and in lipid bilayers studied with FRET

J. Kriegsmann [a], M. Brehs [a], J.P. Klare [b,1], M. Engelhard [b], J. Fitter [a,*]

[a] Forschungszentrum Jülich, INB-2, Biologische Strukturforschung, D-52425 Jülich, Germany
[b] Max-Planck-Institut für Molekulare Physiologie, Otto-Hahn-Str. 11, 44227 Dortmund, Germany

ARTICLE INFO

Article history:
Received 5 August 2008
Received in revised form 10 November 2008
Accepted 10 November 2008
Available online 24 November 2008

Keywords:
Fluorescence spectroscopy
Lipid vesicle
Photo signalling
Sensory rhodopsin
Membrane protein interaction
Dissociation constant

ABSTRACT

The photophobic receptor from *Natronomonas pharaonis* (NpSRII) forms a photo-signalling complex with its cognate transducer (NpHtrII). In order to elucidate the complex formation in more detail, we have studied the intermolecular binding of both constituents (NpSRII and $NpHtrII_{157}$; truncated at residue 157) in detergent buffers, and in lipid bilayers using FRET. The data for hetero-dimer formation of NpSRII/NpHtrII in detergent agrees well with K_D values (~200 nM) described in the literature. In lipid bilayers, the binding affinity between proteins in the NpSRII/NpHtrII complex is at least one order of magnitude stronger. In detergent the strength of binding is similar for both homo-dimers (NpSRII/NpSRII and NpHtrII/NpHtrII) but significantly weaker (K_D ~16 μM) when compared to the hetero-dimer. The intermolecular binding is again considerably stronger in lipid bilayers; however, it is not as strong as that observed for the hetero-dimer. At a molar transducer/lipid ratio of 1:2000, which is still well above physiological concentrations, only 40% homo-dimers are formed. Apparently, in cell membranes the formation of the assumed functionally active oligomeric 2:2 complex depends on the full-length transducer including the helical cytoplasmic part, which is thought to tighten the transducer–dimer association.

1. Introduction

Bacteria and Archaea have to deal with and to respond to very different and extreme environmental conditions. Their evolutionary success for survival is based on their ability to react to altered environmental conditions — genetically or in a fast locomotive action. A prerequisite for an effective response is a molecular apparatus, which is able to receive signals from the environment and transmit this information via the plasma membrane to cellular signalling networks. In general, these machineries are composed of integral membrane proteins. In the case of the archaeon *Natronomonas pharaonis* photo-signalling is triggered by a protein complex consisting of a photoreceptor (NpSRII) and its cognate transducer (NpHtrII) [1–5]. The transducer represents an interface between the transmembrane signalling complex and the cellular chemotactic two component system. Members of this signalling cascade are a histidine kinase CheA and response regulators CheY and CheB. CheA phosphorylates CheY and CheB which function as a switch for the flagellar motor and regulate adaptation, respectively [6,7].

In the present study, the interaction of the receptor with its cognate transducer is analyzed in more detail. Crystal structures at atomic resolution are available for both receptor and receptor transducer complex [8–10]. EPR-spectroscopy studies on the Np(SRII/HtrII)-complex in lipids indicated that NpSRII and NpHtrII are arranged in a 2:2 complex with a two-fold symmetry, which is formed by the transmembrane helices of a transducer dimer [11]. Such an arrangement was confirmed by the X-ray crystal structure of the complex which was obtained by using a truncated transducer analog lacking the cytoplasmic domain [10] (see Fig. 2). This domain has a high sequence homology to corresponding domains of bacterial chemoreceptors [12]. The shortened transducer is still able to bind to NpSRII to form the Np(SRII/HtrII)-complex as was shown by isothermal titration calorimetry [13] (K_D ~200 nM). Contrary to the situation in lipids for which a 2:2 stoichiometry was observed [10,11,14] in detergent only a 1:1 Np(SRII/HtrII)-complex is found [13].

Np(SRII/HtrII) binding has been studied mainly by measuring photocycle properties of NpSRII which are altered upon transducer binding [15,16] and by isothermal titration calorimetry (ITC) [13,17]. Recently also fluorescence spectroscopy (Förster energy resonance transfer) was employed to monitor transducer–receptor binding in detergent [18–20]. To study the transducer/receptor interactions in lipid membrane systems, electron paramagnetic resonance (EPR)

Abbreviations: FRET, Förster resonance energy transfer; NpSRII, *Natronomonas pharaonis* sensory rhodopsin II; $NpHtrII_{157}$, *Natronomonas pharaonis* transducer of sensory rhodopsin II truncated at residue 157, DDM, β-dodecyl-D-maltoside; POPC, palmitoyl oleoyl phosphatidyl choline; LUV, large lamellar vesicle; QY, fluorescence quantum yield; ITC, isothermal titration calorimetry; EPR, electron paramagnetic resonance

* Corresponding author. Tel.: +49 2461 612036; fax: +49 2461 612020.
E-mail address: j.fitter@fz-juelich.de (J. Fitter).
[1] Present address: Universität Osnabrück, Fachbereich Physik, Barbarastrasse 7, 49069 Osnabrück, Germany.

0005-2736/$ – see front matter © 2008 Elsevier B.V. All rights reserved.
doi:10.1016/j.bbamem.2008.11.011

spectroscopy was performed [11,14,21]. With these techniques Np (SRII/HtrII) was studied as densely packed protein complexes (molar protein/lipid ratios of 1:40–1:50). High sensitivity of modern fluorescent probes makes fluorescence techniques ideally suited to perform studies with a broad range of rather different protein concentrations, including extremely low protein concentrations. For various other membrane proteins fluorescence based techniques have been applied successfully to study protein oligomerization at rather low protein/lipid ratios, both in liposomes [22–24] and in cells [25–27]. Our goal is to perform FRET measurements at different protein concentrations in order to estimate the intermolecular binding affinities between proteins in hetero-dimers Np(SRII/HtrII) and in homo-dimers Np(HtrII/HtrII), Np(SRII/SRII) for both environments, detergent and lipid bilayers. Because binding affinities between membrane proteins are assumed to be much stronger in lipid bilayers as compared to detergent [28], the experiments have to be done at very low protein concentrations. The results should provide insights about how protein complex formation is accomplished in cell membranes.

2. Materials and methods

2.1. Protein expression and cysteine mutants

Expression of the photoreceptor NpSRII and the N-terminal fragment of NpHtrII consisting of residues 1–157 ($NpHtr_{157}$), was carried out in *Escherichia coli*. For purification purposes, both proteins carry a C-terminal His_7-tag. Cysteine mutations were introduced using the overlap extension method [29]. Details on protein expression and purification were described in earlier work [11,30]. In brief, transformed *E. coli* BL21(DE3) cells were grown at 37 °C in 2TY medium supplemented with 50 μg/ml kanamycin. At an OD_{578} of 1.0–1.2, 0.5 mM IPTG and for NpSRII 10 mM all-trans retinal were added. After an induction period of 2.5 h, the cells were harvested, washed and resuspended in a phosphate buffer and finally broken up in a microfluidizer (Microfluidics Corporation, Newton, MA). Membranes were sedimented at 100,000 g for 1 h at 4 °C and solubilized in buffer A (2% DDM (Calbiochem), 300 mM NaCl, 50 mM NaP_i, pH 8.0) for 16 h at 4 °C. After centrifugation of the solubilized membranes (100,000 g, 1 h, 4 °C) the supernatant was applied onto a Ni-NTA agarose (Qiagen, Hilden, Germany) chromatography column, washed extensively with buffer B (0.05% DDM, 300 mM NaCl, 50 mM NaP_i, pH 8.0, 20 mM and 80 mM Imidazole for NpSRII and NpHtrII, respectively) and eluted in buffer C (0.05% DDM, 300 mM NaCl, 50 mM Tris–HCl, 150 mM imidazole, 50 mM NaP_i, pH 8.0). Subsequently, the buffer was exchanged to 0.1% DDM, 500 mM NaCl, 10 mM Tris, pH 8.0 using a DEAE ion exchange column.

2.2. Protein labeling with fluorophores

Cysteine mutants were labeled with maleimide functionalized dyes (Atto425 from Atto-Tec GmbH, Siegen, Germany; Alexa532 and Alexa633 from Invitrogen, Karlsruhe, Germany; Cy7Q from Amersham Biosciences, Uppsala, Sweden). Purified protein (2–10 μM) was dialysed against the standard buffer (10 mM Tris–HCl, 150 mM NaCl, 0.05% DDM, pH 7.4) for 24 h. In this buffer a 3–7 fold excess of dye was added to the protein solution and the reaction was carried out overnight at 4 °C. Unbound dye was removed using a gel-filtration column (Sephadex G-25, Amersham Biosciences). In order to determine the label ratio, absorption spectra of all elution fractions were measured using an UV-2401PC spectrometer (Shimadzu, Duisburg, Germany). Protein concentration was determined by measuring the absorption at 280 nm and at 500 nm for the photoreceptors and at two wavelengths around 230 nm for the transducer [13]. To obtain higher protein concentrations for subsequent FRET studies the solutions were concentrated using a 5 kDa cut-off concentrator (Amicon Ultra, Millipore, Carrigtwill, Ireland). Fractions with reasonable label ratios ($1.0 > f > 0.3$) were used for subsequent FRET measurements. Apparent "label ratios" for the retinal chromophore in NpSRII were determined by comparing protein absorption at 280 nm (ε_{max}=49,300 $M^{-1}cm^{-1}$) and retinal absorption at 500 nm (ε_{max}=40,000 $M^{-1}cm^{-1}$). Label ratios of dye labeled photoreceptors, for which the absorption is measured at 500 nm, were determined considering the apparent label ratios of retinal chromophores.

2.3. Preparation of lipid vesicles and reconstitution of proteins into vesicles

Receptor and transducer molecules were reconstituted into POPC liposomes. For this purpose, 5–15 mg POPC (Avanti Polar Lipids Inc., Alabaster, USA) was dissolved in 1 mL chloroform. This solution was transferred into a cleaned glass tube, which was permanently rotated under nitrogen flow. After evaporation of chloroform, a multi-lamellar lipid film was obtained which was dried for at least 2 h under vacuum. Subsequently, the dried lipid film was rehydrated in standard buffer (without detergent). The solution obtained was extruded using a LiposoFast (LF-1) extruder from Avestin (Mannheim, Germany) using polycarbonate membranes with a pore size diameter of 100 nm. The size distribution of lipid vesicles was measured using a DynaPro dynamic light scattering system from ProteinSolutions (Lakewood, NJ, USA). The membrane protein reconstitution into liposomes was performed using Bio-beads (Bio-Rad Laboratories, München, Germany). First, membrane proteins (in detergent buffer) and liposomes were mixed at molar protein/lipid ratios between 1/2000 and 1/8000. In order to initiate detergent extraction, we added 750 mg Biobeads to 1 mL of the protein/lipid mixture. After 2 h, we extracted the resulting proteoliposomes with a glass pipette. Finally, the proteoliposomes obtained were analyzed again with dynamic light scattering for size distribution. Typically the unimodal size distribution of the vesicles with a maximum around R_H=60–80 nm did not change after the reconstitution. Final absorption measurements reveal a protein loss between 20 and 40% for labeled proteins (NpSRII and NPHtrII) upon reconstitution into liposomes. The loss of phospholipids during reconstitution with Biobeads was estimated to be in the range of 20–30% [31]. Based on this information, we assume that the initial protein/lipid ratios are not altered significantly during the reconstitution and therefore have used the initial protein/lipid ratios for all further calculations.

2.4. Calculation of protein surface density

In order to compare FRET efficiencies of proteins dissolved in detergent buffer with those embedded in lipid bilayers, we calculated the averaged distance between next neighbors. Lipid vesicles with an average radius of 70 nm produce a surface area of about 6,160,000 $Å^2$. Assuming a surface area of 72 $Å^2$ per lipid molecule [32] a single vesicle consists of approximately 170,000 lipids. For protein/lipid ratios of 1:2000, 1:4000 or 1:8000 and assuming random distribution among all vesicles one should have 84, 42, and 21 proteins per vesicle, respectively. From this we calculated averaged next neighbor distances, which are 270 Å, 380 Å or 540 Å, respectively. For proteins in solution (3D distribution), one can calculate averaged next neighbor distances simply on the basis of the protein concentration.

2.5. Fluorescence techniques

Fluorescence emission spectra were obtained using a QuantaMaster spectrofluorometer (QM-7) from Photon Technology International (Lawrenceville, NJ, USA). The instrument was equipped with a constant temperature cuvette holder, with a pair of Glan–Thomson polarizers, and with a long wavelength sensitive photomultiplier

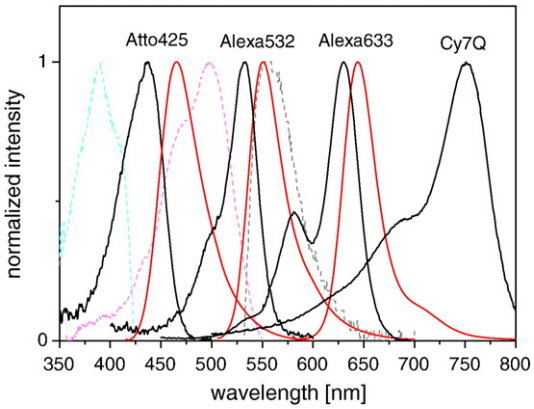

Fig. 1. Normalized absorption (black lines) and fluorescence emission spectra (red lines) of the dyes used in this work. In addition, the normalized absorption of the retinal chromophore as bound to the protein (dotted lines) is shown for the ground state (violet), for the M-state (blue), and for the O-state (gray). The following values for chromophores were used: Atto425, ε_{max}: 45,000 $M^{-1}cm^{-1}$, QY: 0.86; retinal Chromophore (ground state): ε_{max}: 40,000 $M^{-1}cm^{-1}$; Alexa532, ε_{max}: 81,000 $M^{-1}cm^{-1}$, QY: 0.82–0.87; Alexa633, ε_{max}: 164,500 $M^{-1}cm^{-1}$, QY: 0.24–0.28; Cy7Q, ε_{max}: 100,000 $M^{-1}cm^{-1}$. The given quantum yields were measured for the dyes bound to the individual cysteine mutants using standard procedures (see for example [22,23]).

(R928, Hamamatsu) to measure dyes emitting in the far red. Samples were measured in semi-micro cells or in ultra-micro cells (104F-QS and 105.251-QS, respectively, both Hellma GmbH, Muehlheim, Germany). Slit widths for excitation and emission wavelengths were varied between 1–5 mm. Fluorescence emission intensities were corrected for background intensities as measured with pure buffer solutions and for inner filter effects considering the corresponding absorption spectra [33]. In the case of proteins reconstituted into liposomes, the scattering background was fitted and thereafter subtracted from the measured spectra.

2.6. FRET measurements

For all FRET measurements we used three different samples, namely a sample containing only donor labeled molecules, one containing only acceptor labeled molecules, and one with donor and acceptor labeled molecules (FRET sample). In a first set of measurements with detergent solubilized proteins, small volumes of highly concentrated acceptor labeled protein (20–25 μM) were added stepwise to a solution of donor molecules (at a concentration of about 2 μM). After an equilibration time of about 30 min, we excited at the respective donor absorption wavelength (λ_{exc}: 420 nm for Atto425, 490 nm for Alexa532, and 570 nm for Alexa633) for each titration step. From the emission spectra we obtained the fluorescence emission intensities of the donor and of the acceptor at the corresponding peak maxima. In a second set of experiments, we mixed donor labeled molecules (at a concentration of about 4 μM) and acceptor labeled proteins at various molar acceptor/donor ratios ranging from 1:0.02 to 1:3. After equilibration for time periods ranging from 10 min to 24 h, fluorescence emission intensities were measured.

Subsequently, all three samples (donor only, acceptor only, and FRET sample) were used for reconstitution into lipid vesicles. For all reconstituted membrane proteins we measured fluorescence emission spectra as described above for the detergent solubilized samples. In addition absorption spectra were measured for all samples employed in fluorescence studies (see legend Fig. 1) in order to correct for inner filter effects and to calibrate the fluorescence intensities with respect to the actual protein concentrations. This was particularly important for the lipid samples where losses of protein during reconstitution could not be avoided. Acceptor emission intensities obtained from FRET samples were corrected for direct excitation of the acceptor emission at the donor excitation wavelength, where the control was a sample containing only acceptor labeled protein. All fluorescence measurements were performed in standard buffer (10 mM Tris–HCl, 150 mM NaCl, 0.05% DDM, pH 7.4). For proteins in lipid bilayers the same buffer was used without the addition of DDM. All measurements were done at room temperature (25 °C).

2.7. Theoretical and measured FRET efficiencies

Based on the 3D structure of the NpSRII/NpHtrII-complex (PDB code: 1H2S [10]) distances R between positions of site specifically labeled dyes were estimated (see Fig. 2). The theoretical FRET efficiencies (E_{theo}) for complexes with labeled proteins are given by:

$$E_{theo} = \left(\frac{R_0^6}{R_0^6 + R^6}\right) = \left(\frac{1}{1 + \left(\frac{R_0}{R}\right)^6}\right) \quad (1)$$

The corresponding Förster radius R_0 is calculated by

$$R_0 = \left(8.79 \cdot 10^{-5} \cdot n^{-4} \cdot \Phi_D \cdot J(\lambda) \cdot \kappa^2\right)^{1/6} \quad (2)$$

and is determined by the overlap integral $J(\lambda)$, the donor quantum yield Φ_D, the refractive index n, and the orientation factor κ^2 (for more details see [33]). The typical value for the orientation factor 2/3 is based on the assumption that bound fluorophores can perform free reorientation movements. Therefore, we measured the steady-state

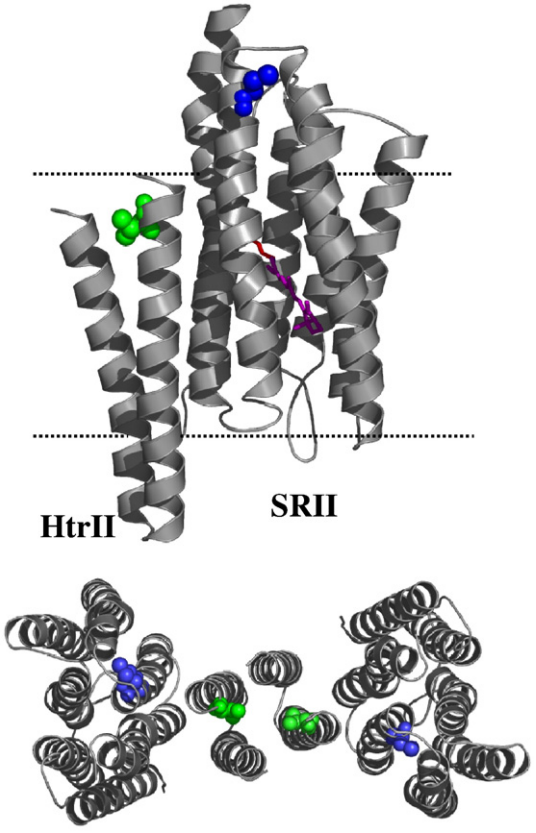

Fig. 2. Schematic presentation of the NpSRII/NpHtrII-complex structure. According to the original data (PDB code: 1H2S) the structure of the transducer is known only for the N-terminal part of NpHtrII up to residue 82. The dotted lines indicate tentatively the lipid bilayer interfaces. The positions of the retinal chromophore (magenta), of mutants NpHtrII–V78C (green), and of NpSRII–K157C (blue) are highlighted. The presentation was produced using PyMOL (DeLano, W.L. The PyMOL Molecular Graphics System (2002) DeLano Scientific, San Carlos, Ca, USA).

Table 1
List of theoretical FRET efficiencies for employed FRET pairs as calculated on the basis of Eq. (2) and using the spectral information given in Fig. 1

FRET pairs	D–A distance[a] R [Å]	Intergral $J(\lambda)$ [$M^{-1}cm^{-1}$ nm^4]	Orientation factor[b] κ^2	Förster radius R_0 [Å]	Efficiency E_{theo}
Atto 425–Ret(G)	30	$1.4985 \cdot 10^{15}$	1/3	48.2	0.945
			4/3	60.7	0.986
Alexa 532–Alexa 633	40	$4.7672 \cdot 10^{15}$	2/3	65.6	0.951
Alexa 532–Ret(G)	30	$1.6345 \cdot 10^{14}$	1/3	33.3	0.652
			4/3	41.9	0.882
Alexa 633–Cy7Q	40	$6.0839 \cdot 10^{15}$	2/3	56.9	0.892

[a] The donor–acceptor (D–A) distances (here for NpHtrII–V78C and NpSRII–K157C positions and for NpHtrII–V78C position and the retinal at ground state conditions, Ret (G)) include a considerable uncertainty due to the spatial extension of the dye molecules (up to 10 Å) and due to the relative orientation of the bound dyes to each other. The respective values given here represent an upper limit of the real D–A distances. Distances obtained from other mutants employed for hetero-pairs (NpHtrII–A94C bound to NpSRII–S154C) and from all homo-pairs (which might be on average slightly smaller) are rather similar within the limits of uncertainty.

[b] The orientation factors for dye pairs were assumed to be 2/3, while for dye-retinal pairs (with a fixed orientation of the retinal) a lower (1/3) and an upper limit (4/3) was used [33].

anisotropy of membrane proteins with cysteine coupled dyes which yield anisotropy values between 0.18–0.22. The expected error in FRET efficiencies due to this deviation from freely rotating dyes is at most 15%–20%, but most likely much smaller (see [23]). The calculations of Förster radii and FRET efficiencies, as well as all other data analysis and data presentation have been accomplished using Origin7.5 (OriginLab Corp., Northhampton, MA, USA). Fluorescence emission intensities I were measured for samples containing only donor labeled proteins (I_D), only acceptor labeled proteins (I_A), and donor labeled proteins in the presence of acceptor labeled proteins (I_{DA}). The resulting measured FRET efficiency E_{meas} due to protein–protein binding is given by:

$$E_{meas} = \frac{1}{FL} \cdot \left(1 - \frac{I_{DA}}{I_D}\right) \tag{3}$$

FL is taking into account label ratios and concentrations of the employed proteins. In the case of FRET studies with hetero-dimerization (i.e. NpSRII/NpHtrII) FL is simply f_A, where f_A is the label ratio of the acceptor. The derivation of FL for hetero- and homo-dimerization, is given in the Appendix. In order to demonstrate the consistence and the validity of the FRET approach we measured in some cases the energy transfer efficiency ratiometrically from donor and acceptor emission intensities [34]:

$$E_{meas}^{ratio} = \frac{1}{FL} \cdot \left(\frac{I_A}{I_A + \gamma \cdot I_{DA}}\right) \tag{4}$$

Here $\gamma = \eta_A \Phi_A / \eta_D \Phi_D$ is a correction factor which considers differences in the detector efficiency η at different wavelengths and in the respective quantum yields Φ of donors and acceptors.

2.8. Calculation of dimer fractions and dissociation constants from FRET efficiencies

For the calculation of the theoretical FRET efficiencies, we assumed that each donor labeled molecule is bound to an acceptor labeled molecule. Therefore, the ratio E_{meas}/E_{theo} gives the normalized fraction of dimers[2] formed. According to the law of mass action the equilibrium reaction is given by D+A↔DA (D: donor labeled monomer; A: acceptor labeled monomer, DA: dimer). The dissociation constant K_D was determined using the following equation:

$$\frac{[DA]}{[DA] + [D]} = \frac{1}{1 + \frac{K_D}{[A_t]}} = \frac{E_{meas}}{E_{theo}} \tag{5}$$

where A_t equals to the total amount of acceptor labeled proteins.

3. Results

For the study of membrane protein interactions, we used three different FRET pairs. In Fig. 1 the corresponding absorption and fluorescence emission spectra of all employed dyes, as well as photoreceptor absorption spectra of the ground state and of two intermediate states are shown. Fig. 2 shows the structure of the complex as known from X-ray crystallography [10]. Based on this structure, distances between positions of the mutated cysteines (highlighted in the respective protein molecules) were obtained. The corresponding theoretical FRET efficiencies (see Materials and methods, Eq. (1)) were calculated for the FRET pairs as given in Table 1.

3.1. Protein labeling

In order to calculate reliable FRET efficiencies, precise values of the label ratio in particular for the acceptor dye (see Materials and methods Eqs. (3), (4) and Appendix A) are essential. For both membrane proteins (NpSRII and NpHtrII) we employed two different *Cys* mutants (see Table 2). The protein concentration of the receptor was determined most precisely by measuring the retinal absorption at 500 nm. Therefore, in hetero-dimerization studies the receptor carried the acceptor. Results obtained from protein labeling and subsequent purification are given in Fig. 3 and Table 2. Respective absorption spectra from different elution fractions (Fig. 3a and b) showed that multiple purification steps (in some cases up to four steps) are necessary to remove unbound dye. An independent measure for an estimation of protein bound label is possible from the observation that in all cases the dyes experiences a small red shift (1–4 nm) when bound to the protein. The label ratios are listed in Table 2.

3.2. NpSRII/NpHtrII binding measured with different FRET pairs

In order to check the suitability of the chosen FRET pairs, we analyzed the photoreceptor/transducer complex (hetero-dimer) formation in detergent buffer with donor and acceptor labeled proteins (concentration 1.5–2 μM) at different molar acceptor/donor ratios. The corresponding fluorescence emission spectra and FRET efficiencies are presented in Fig. 4. We observe a characteristic decrease of the donor intensity upon increasing acceptor concentration (Fig. 4a, c, and e). Fig. 4c shows for the Alexa532/Alexa633 pair concomitantly with the donor intensity decrease an increase of the acceptor emission intensity, which is an additional signature for FRET. In the case of the photoreceptor retinal chromophore (almost non-fluorescent) and of

Table 2
List of obtained label ratios

	Retinal	Atto 425	Alexa 532	Alexa 633	Cy7Q
$NpHtrII_{157}$–V78C		0.60–0.95	0.50–0.95	0.45–0.75	
$NpHtrII_{157}$–A94C			0.50–1.00	0.40–0.85	0.85–0.98
NpSRII–K157C	0.72–0.75			0.40–0.80	0.40–0.93
NpSRII–S154C	0.70–0.75			0.60–0.78	
NpSRII–wt	0.80				

[2] In principle, our data cannot discriminate between the formation of dimers and higher-order oligomers. However, based on the knowledge from the literature [13,15,18] we have restricted our interpretation for hetero pair as well as for homo-pair binding to dimeric interactions.

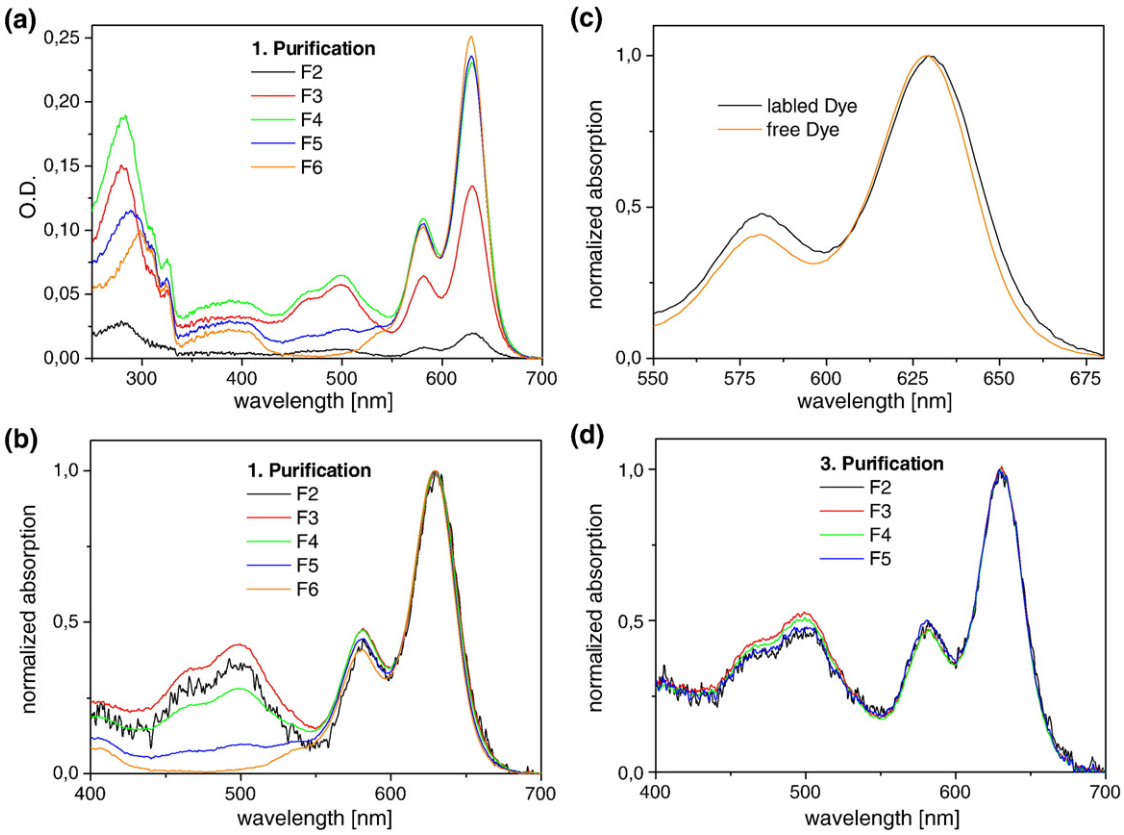

Fig. 3. Absorption spectra from elution fractions of NpSRII reacted with Alexa633 as obtained from purifications using a gel filtration column. (a) The five absorption spectra on the absolute scale show protein chromophore absorption (λ_{max}: 500 nm) and dye absorption (λ_{max}: 630 nm) to different extents. Elution fractions F3 and F4 contain the major absolute amount of protein, while fraction F5 includes already a larger fraction of free dye. Finally, F6 represents only free dye. (b) The normalized spectra of the data shown in (a) clearly demonstrate that the major protein fraction (F3 and F4) exhibit rather different label ratios indicating that at least one elution fraction still contains free dye. (c) The comparison between free Alexa633 and the same dye bound to the protein exhibits small spectral differences with respect to λ_{max} and to intensities in a shoulder around 580 nm. (d) After the 3rd purification the elution fractions (F2–F5) are homogenous within the limits of error and contain no longer free dye. Qualitatively the observations made for the sample shown in this figure (a–c) were also found for the other protein dye conjugates.

the Cy7Q (mainly an absorber or quencher) as acceptor molecules, the acceptor emission is either absent (Fig. 4a) or very weak (Fig. 4e). From the measured fluorescence emission intensities we calculated the corresponding FRET efficiencies using Eqs. (3) and (4) (Fig. 4b, d, and e). For all FRET pairs these efficiencies increase with a larger molar acceptor/donor ratio and saturate at acceptor/donor ratios of about two at the level of the corresponding calculated efficiency levels (dashed lines in Fig. 4b, d, and f, see figure legend). In the case of the Alexa532/Alexa633 pair we also determined ratiometrically measured efficiencies (open symbols in Fig. 4d, Eq. (4)) which, within the limits of error, coincide with those obtained using only donor intensities (solid symbols using Eq. (3)).

Based on this data we can state the following about the receptor/transducer complex formation in detergent buffer: (1) Receptor/transducer binding shows a strong dependence on the stoichiometric relation of the binding partners. At a donor concentration of 1.5–2 μM and with acceptor molecules in two fold-excess we observed that approximately 80% of all transducers are bound to their respective partner molecule (receptor). (2) All employed FRET pairs exhibit the same results and appear to be applicable for binding studies. This indicates that dyes, when bound to proteins, do not significantly hinder the complex formation. Furthermore, photocycle activation (occurring for two FRET pairs, either due to energy transfer to the retinal or due to direct excitation at donor excitation wavelength of ~500 nm) seems not to hamper or suppress receptor/transducer binding. This is indicated by the fact that we observe the same binding behavior for measurements with and without photocycle excitation (compare Fig. 4d, and d with Fig. 4f). Further measurements with the other mutants (NpSRII-S154C and NpHtrII-A94C, data not shown) reveal nearly the same results as compared to those presented in Fig. 4.

3.3. Formation of hetero-dimers and homo-dimers in detergent and in lipids

The following measurements aim to investigate differences in protein binding between proteins in detergent buffer and proteins embedded in lipid bilayers using mainly the Alexa532/Alexa633 FRET pair. For this dye combination, the fluorescence emission intensities were sufficiently large even with respect to strong scattering observed for samples in lipid vesicles. The Np(SRII/SRII) homo-dimer formation had to be investigated with the Alexa633/Cy7Q FRET pair because only for this pair the energy transfer to the receptor retinal is absent.

In first measurements on Np(SRII/HtrII) binding with a molar ratio of 1:1, we obtained FRET efficiencies of about 0.5 (see Table 3). These results contradict previous studies, that at protein concentrations of about 4 μM the FRET efficiency reaches its maximum level at a molar ratio of 1:1 [18,19]. A reason for this discrepancy could be that apparent association constants of membrane proteins are strongly effected by detergent concentration [35,36]. In order to ensure FRET measurements at defined detergent concentrations, we dialyzed purified protein samples for 16 h against standard buffer containing 0.05% DDM. Under these conditions, protein mixtures with a molar ratio 1:1 reached almost the highest possible FRET efficiencies (see Table 3 and Fig. 5a).

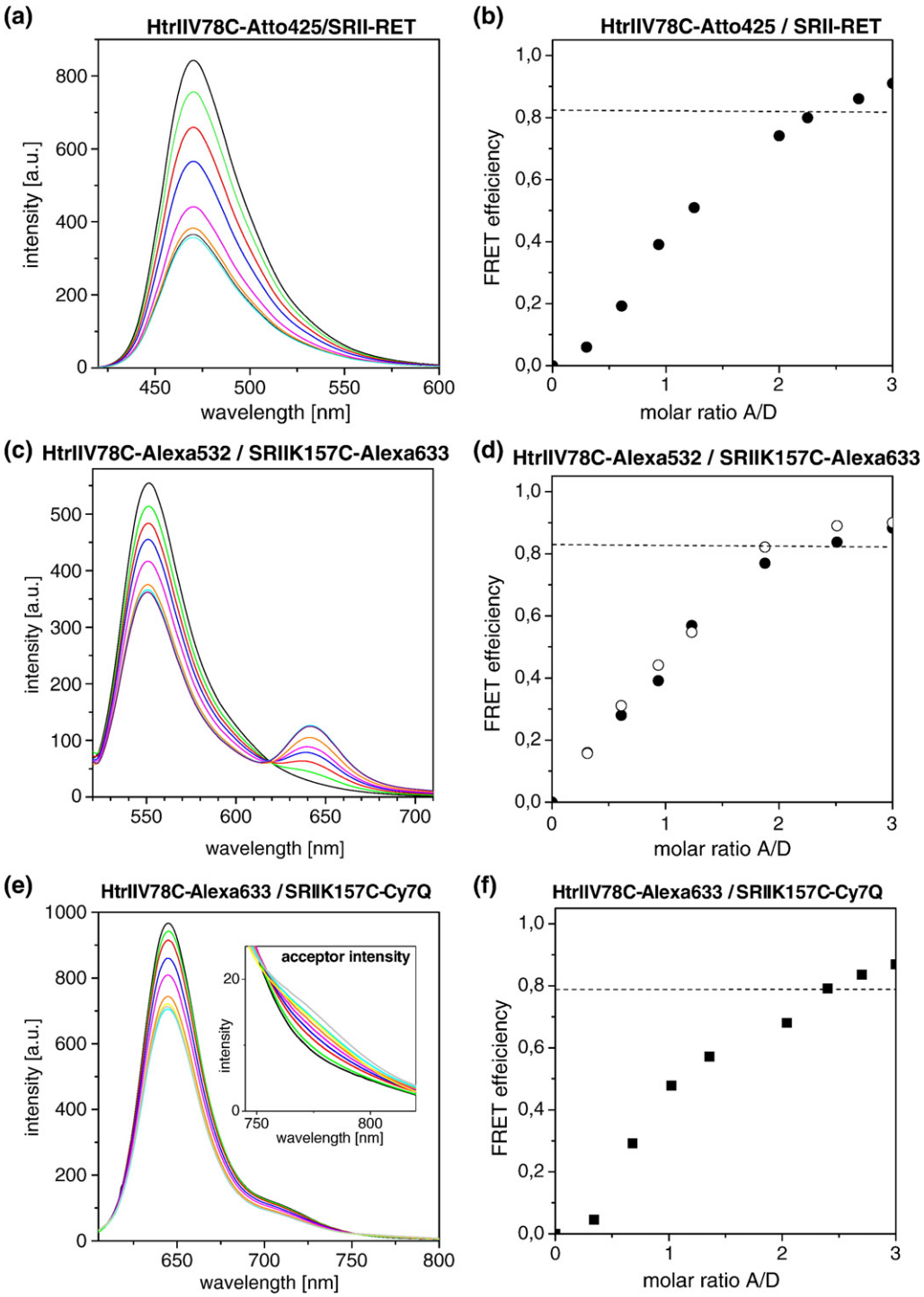

Fig. 4. Measured fluorescence emission spectra (a, c, and e) for three different FRET pairs. Highly concentrated solutions of acceptor molecules have been titrated to a solution containing donor molecules at a concentration of 2 μM. With increasing acceptor concentration, the donor emission intensity decreases due to energy transfer. In cases where Alexa633 or Cy7Q was used as acceptor, the accompanying increasing acceptor intensity is visible around 645 nm for Alexa633 (see panel c) and around 775 nm for Cy7Q (see inset of panel e). The corresponding measured FRET efficiencies are given as a function of the molar acceptor/donor ratio (b, d, and f). The dashed lines in these panels represent calculated FRET efficiencies as assumed for the case that 80% of all transducer are bound to a receptor (which is expected for a K_D of about 200 nM at 2 μM donor concentration [13]). The presented FRET efficiencies (see Materials and methods) were calculated using Eq. (3) (solid symbols) and in addition using Eq. (4) (open symbol, only for the case shown in panel d).

If lipid bilayers were used to study protein binding, we applied protein/lipid ratios between 1:2000 and 1:8000. In the case of hetero-dimer formation (1:1 molar donor/acceptor ratio) we observed FRET efficiencies between 0.8–0.9 for all protein lipid ratios, indicating that under these conditions all possible NpHtrII/NpSRII pairs have been formed (Fig. 5b). In contrast, homo-dimers showed much smaller FRET efficiencies for both detergent and lipid samples (see Fig. 6 and Table 3). NpHtrII/NpHtrII binding exhibits FRET efficiencies of about 0.2 for a molar ratio of 1:1 and around 0.4 for a molar ratio of 1:3 in detergents. In lipids FRET efficiencies of about 0.4 were measured for a protein/lipid ratio of 1:2000 and at a molar donor/acceptor ratio of 1:1. In order to ensure that dyes bound to the transducer do not hinder a proper homo-dimer formation we used combinations of two different transducer mutants (NpHtrII–

Table 3
Obtained FRET efficiencies for different protein binding properties

Pair	Molar donor–acceptor ratio	Donor protein concentration [μM][b]	Environment	Efficiency[a] E_{meas}
Hetero pair				
NpHtrII–NpSRII	1:1	3.5–4.7	Detergent >0.05%	0.52±0.03
NpHtrII–NpSRII	1:3	3.5–4.7	Detergent	0.84±0.08
NpHtrII–NpSRII	1:1	3.8–4.5	Detergent	0.85±0.07
NpHtrII–NpSRII	1:1	0.5–1.5 1:2000	Lipid	0.87±0.07
NpHtrII–NpSRII	1:1	0.6–1.5 1:4000	Lipid	0.89±0.05
Homo pairs				
NpHtrII–NpHtrII	1:1	3.7–4.9	Detergent	0.20±0.02
NpHtrII–NpHtrII	1:3	3.5–4.2	Detergent	0.39±0.03
NpHtrII–NpHtrII + NpSRII[c]	1:1:2	3.6–4.2	Detergent	0.23±0.03
NpHtrII–NpHtrII + NpSRII[d]	1:1:2	3.4–4.1	Detergent	0.86±0.07
NpHtrII–NpHtrII	1:1	0.7–1.2 1:2000	Lipid	0.41±0.04
NpHtrII–NpHtrII + NpSRII[c]	1:1:2	0.4–1.2 1:2000	Lipid	0.39±0.03
NpSRII–NpSRII	1:1	3.5–4.2	Detergent	0.23±0.03
NpSRII–NpSRII	1:3	3.8–4.6	Detergent	0.38±0.02
NpSRII–NpSRII	1:1	0.8–1.3 1:2000	Lipid	0.32±0.04
Weak binding pair[e]				
NpHtrII–BR	1:3	3.2–4.4	Detergent	0.04±0.02
NpHtrII–BR	1:3	0.6–1.3 1/2000	Lipid	0.03±0.02

[a] The given values and the corresponding standard deviations were obtained from 3–6 independent measurements for each pair. The following FRET pairs were employed: Hetero pair with Alexa532–Alexa633; Homo pairs: NpHtrII–NpHtrII with Alexa532–Alexa633 and NpSRII–NpSRII with Alexa633–Cy7Q.
[b] For all lipid samples in addition, the more relevant molar protein/lipid ratio is given.
[c] Unlabeled receptor.
[d] Acceptor labeled receptor.
[e] BR wildtype (acceptor) with a retinal absorption peak maximum at λ_{max}=568 nm (ε_{568}: 63,000 $M^{-1}cm^{-1}$) and NpHtrII labeled with Alexa532 (donor) were employed as FRET pair with a Förster radius R_0=66.7 Å and a theoretical FRET efficiency of E_{theo}=0.99.

V78C, NpHtrII–A94C). For all possible combinations of NpHtrII mutants we obtained approximately the same FRET efficiencies. Remarkably, even NpSRII/NpSRII homo-dimers were formed with similar efficiencies in detergent and in lipids as compared to those observed for the NpHtrII/NpHtrII homo-dimer. Using FRET efficiencies measured at different concentrations of acceptor labeled proteins the corresponding dissociation constants were calculated using Eq. (5). For hetero- and homo-dimerization in detergent the results are shown in Fig. 7.

In order to check whether the observed FRET signals originate from specific binding (in particular for the homo-dimers), we performed a series of measurements with stepwise diluted FRET samples. For this purpose, we diluted selected detergent samples 20- to 100-fold with detergent buffer. The FRET efficiencies approached very small values (data not shown) within minutes indicating complete dissociation upon dilution to protein concentrations below the K_D. This behavior is characteristic for a specific and reversible binding process, unlike an often observed unspecific and irreversible aggregation process. A further control check was performed with bacteriorhodopsin (BR) as a potential binding partner for NpHtrII. As known from recent ITC studies, the binding of BR to NpHtrII is rather weak with a K_D>300 μM in detergent [17]. Therefore, we expect very small FRET efficiencies for this pair at protein concentrations of about 4 μM, which is indeed observed (see Table 3). Also in lipids a BR/NpHtrII binding is negligible.

In a further series of measurements, we analyzed the competition between homo-dimer and hetero-dimer formation in detergents. For this purpose, we prepared a homo-dimer sample (1:1 molar ratio) of NpHtrII and measured the FRET. Subsequently we added the same amount of NpSRII (either acceptor labeled or non-labeled) to the sample and analyzed the sample for changes in the FRET efficiency. In the case of labeled NpSRII, we observed a significant increase of the FRET efficiency (see Fig. 6a, red dashed line). The additional hetero-dimer formation contributes considerably to the observed FRET efficiencies, which are quite similar to those observed for the hetero-pair binding. The experiment with unlabeled NpSRII was performed with Alex633/Cy7Q pair in order to avoid energy transfer to the receptor retinal chromophore. Upon adding unlabeled NpSRII to NpHtrII the FRET signal is almost unchanged (see Table 3). Also in lipid bilayers, the presence of NpSRII does not affect NpHtrII/NpHtrII binding significantly. These observations give rise to the following conclusions. Hetero-dimer formation seems not to be competitive with homo-dimer binding. We do not have indication that hetero-binding is replacing or enhancing homo-pair binding of NpHtrII. Similar results were obtained also for NpSRII/NpSRII homo-pair binding, where we employed unlabeled NpHtrII as competitor.

4. Discussion

Since detailed knowledge about the strength of NpHtrII/NpSRII hetero-dimer binding in detergent buffers is known from the literature we first studied this interaction to calibrate our methodical approach. As shown in Fig. 7, we obtained fractions of bound acceptor molecules which agree reasonably well with the K_D of about 200 nM as determined earlier with ITC in detergent buffer [13].

A comparison of results obtained from detergent samples with those from lipid bilayers is not straightforward and needs a consideration of the following aspects. (1) The concentrations of proteins in detergent buffer as well as in lipid vesicles have to be sufficiently low so that the averaged mean distance (nearest neighbor distance) is much larger than the Förster radius (~50–60 Å). For mean distances Δr reaching the regime of the Förster radius, FRET can arise simply due to random proximity of the acceptors and donors (see for example [37]). The highest protein concentration in detergent used in this study corresponds to an average mean distance of about 450 Å (see Materials and methods). In lipid systems, which form two dimensional planes essentially the protein/lipid ratio determines the mean distance, which is about 270 Å for a concentration of one mole of protein molecules per 2000 mol of lipid molecules. Therefore, under the conditions used in this work we can assume that the observed FRET is caused predominately by intermolecular protein binding. (2) It is evident from the calculated average mean distances between neighboring proteins that in the lipid samples higher apparent protein concentration than in the detergent sample are readily achieved. This is caused by the fact that in the lipid bilayers proteins are distributed on the surface of a spherical liposome (2D space), while for the detergent samples the proteins are spread within a volume (3D space). In order to compare the strength of protein–protein binding in detergent and in lipid samples we have to compare the collision frequencies in both systems. This parameter determines how often both binding partners meet each other and have the chance to form a complex. In detergent buffer micelles, typically carrying one membrane protein, have to fuse with another micelle or protein exchange between micelles has to take place. Essentially, the collision frequency

is determined by the mean distance between adjacent proteins and the diffusion time (t) of the membrane proteins. The latter can be calculated by

$$t = \frac{\langle \Delta r \rangle^2}{6D_{3D}} \text{ and } t = \frac{\langle \Delta r \rangle^2}{4D_{2D}} \quad (6)$$

for the case of 3D and 2D diffusion, respectively. Diffusion coefficients of NpHtrII or NpSRII in detergent micelles ($D_{3D} \sim 7 \cdot 10^{-7}$ cm^2/s) are much larger than corresponding values obtained for diffusing proteins in lipid bilayers ($D_{2D} \sim 4 \cdot 10^{-8}$ cm^2/s, Kriegsmann et al., unpublished results). One approach to estimate the binding affinity of membrane proteins in lipid bilayers is to compare measured FRET efficiencies at conditions where collision probabilities are the same for detergent and lipid samples. According to Eq. (6), membrane proteins in a sample with protein/lipid ratio of 1:2000 have the same collision probability as proteins in detergent at a concentration of 0.32 μM. Protein/lipid ratios of 1:4000 and 1:8000 correspond to a protein concentration of 0.11 μM and 0.04 μM, respectively.

Taking these considerations into account, we observe for the hetero-dimers significant differences in FRET efficiencies between detergent and lipid samples. While for the detergent samples the measured FRET efficiencies are decreasing drastically with decreasing protein concentrations (which is expected for a K_D of 0.2 μM, see Fig. 7), the corresponding FRET efficiencies for proteins in lipid bilayers remain constantly high ($E_{meas} \approx 0.8$–0.95; see Table 3) even for the lowest protein concentration (protein/lipid ratio 1:8000, data not shown). From these observations, we can estimate that in lipid bilayers the binding affinity between NpSRII and NpHtrII is at least one order of magnitude stronger as compared to proteins in detergent[3]. Samples with even smaller protein/lipid ratios cannot be analyzed with this experimental approach due to stronger relative contributions from scattering. However, most probably the hetero-pair binding is much stronger than indicated by our estimation. Measurements with proteins in giant unilamellar vesicles (20–50 μM in diameter) with protein/lipid ratios in the order of 1:1,000,000 reveal NpHtrII/NpSRII binding (Kriegsmann et al., unpublished results).

As known from the structure of the receptor/transducer complex [10], Tyr 199 and Thr 189 located in helix G of NpSRII play a crucial role for the strength of transducer binding. In particular, hydrogen bonds and aromatic side-chain interactions are supposed to be responsible for the relative strong NpSRII/NpHtrII binding [13,17]. However, the much stronger NpSRII/NpHtrII binding in lipid bilayers as compared to the detergent environment is most probably caused by the effect of pre-oriented membrane proteins in the lipid bilayers in contrast to randomly oriented proteins in detergent. Due to the more or less parallel and uniform orientation of all membrane proteins with respect to the bilayer vertical reference line, any collision of diffusing proteins can lead to a drastically higher probability of dimerization [28]. Another possible reason for higher binding affinities in lipid bilayers might be related to thermodynamics. It is known from thermodynamic data that NpSRII/NpHtrII binding is significantly mediated by entropic contributions [17]. Before receptor/transducer binding can take place, detergent and lipid molecules need to be removed from the binding interface. The (entropic) energy required for this removal may be much higher for detergent molecules as compared to lipids, which form a bilayer.

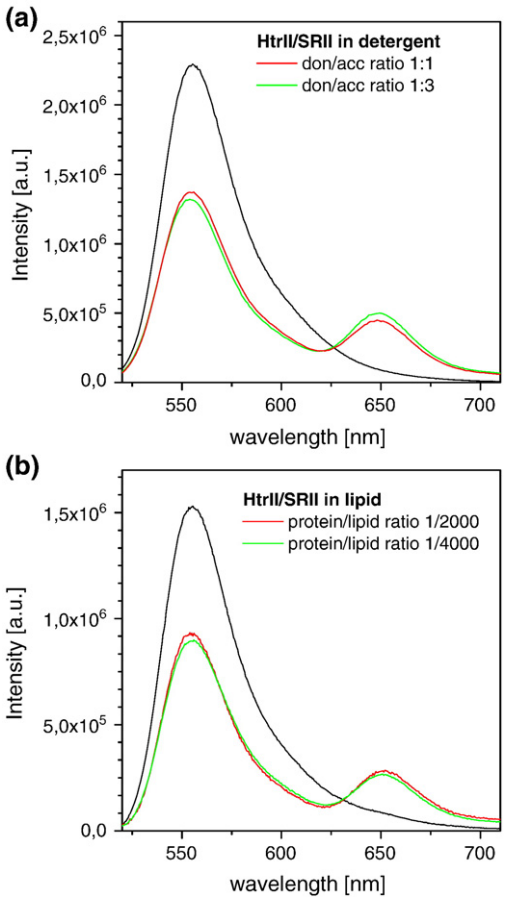

Fig. 5. Fluorescence emission spectra are shown for NpHtrII/NpSRII samples measured in detergent (a) and in lipid bilayers (b). Black lines represent spectra of samples containing only donor labeled molecules. They serve as a reference for FRET samples with different molar donor/acceptor ratios and with different protein/lipid ratios. The corresponding FRET efficiencies are given in Table 3.

In contrast to the NpHtrII/NpSRII binding, which was investigated already in detergent in various studies, little is known about the strength of homo-dimer formation. Some recent studies report a weak binding of homo-pairs in detergent [13,38,39]. Our data reveal that for both homo-pairs the intermolecular binding is characterized by significantly smaller FRET efficiencies as compared to corresponding values for hetero-pairs. In addition, the increase of FRET efficiencies with increasing protein concentrations in detergent is rather small. Therefore, the obtained K_D values for both homo-pairs in detergent are only in the order of 16 μM (see Fig. 7). Remarkably, FRET efficiencies for both homo-pairs in lipids exhibit similar values as observed for samples measured in detergent buffer. For a protein/lipid ratio of 1:2000 we observe that only 40% of all transducer molecules form homo-dimers. This fraction is slightly smaller for receptor homo-dimers (30–40%). Again, based on different collision probabilities as observed in detergent samples (protein concentration 4 μM) and in lipid samples (protein/lipid ratio of 1:2000), we can state a much stronger homo-dimer binding in lipids as compared to detergent (approximately by one order of magnitude). To summarize, we can conclude that binding affinities obtained for membrane proteins in detergent are significantly smaller than those obtained from lipid samples. Our results therefore indicate that K_D values measured in detergent buffers are rather limited in their informational value for

[3] For the sample with the lowest protein/lipid ratio (1:8000), the normalized fraction of dimers FD ≈ 0.9 was obtained at the equivalent concentration of acceptor labeled proteins [A_t] of 0.04 μM. According to Eq. (5) we would obtain an apparent $K_D = (1/FD-1) \cdot [A_t] = 0.0044$ μM. This value is smaller by a factor 45 as compared to 0.2 μM which was observed for samples in detergent. This calculation gives only a rough and qualitative estimate of the lower limit of the increase in protein binding occurring in lipid bilayers. For example, lifetimes of the encounter-complexes are not considered and lower protein/lipid ratios required for a more meaningful titration are experimentally not accessible.

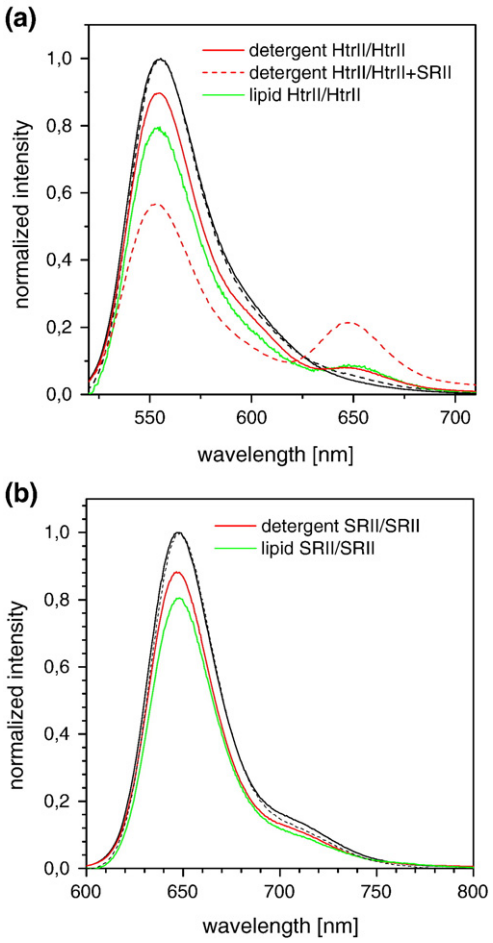

Fig. 6. Measured fluorescence emission spectra are shown for NpHtrII/NpHtrII (a) and NpSRII/NpSRII (b) homo-dimers. Black lines represent emission spectra of samples with only donor labeled proteins (solid line: in detergent; dashed line: in lipids). For spectra shown here, the donor/acceptor ratio was 1:1. For the NpHtrII/NpHtrII + NpSRII (acceptor labeled) sample ratios were 1:1:2 (see also Table 3).

characterizing the strength of intermolecular membrane protein binding in cell membranes and only provide a relative prediction.

In contrast to the receptor/transducer hetero-pair, specific contacts between two transducer molecules (homo-dimer) have not been identified in the structure of the complex. This is the reason why binding affinities between proteins in homo-dimers are in general much weaker as compared to hetero-dimers. However, earlier studies on the NpHtrII/NpHtrII homo-dimer formation in lipid bilayers revealed evidence for a stronger binding which is in accordance with a more or less stable 2:2 complex [10,11,13,21]. Most probably, this difference (to our results) stems from the fact that in all previous studies much higher molar protein/lipid ratios (1:40–1:50) were employed. With these protein/lipid ratios the observed NpHtrII/NpHtrII binding can be the result of packing effects. The fact that we observe only 40% of transducer homo-dimers are formed at a protein/lipid ratio of 1:2000 (which is still well above physiological transducer/lipid ratios in the cell membrane; Otomo et al. estimate ~400 photoreceptors per cell [40]) indicates that under physiological conditions the membrane embedded and the membrane adjacent part of the transducer (N-terminal part up to a length of 157 residues) are not sufficient to form stable and long-lasting NpHtrII/NpHtrII contacts which are assumed to be a prerequisite for forming the 2:2 complex. Therefore, assuming that the 2:2 complex is the functional unit for the signalling complex, a stronger and long-living NpHtrII/NpHtrII contact seems to require the full-length transducer. The coiled-coil structure of the four-helix bundle of the cytoplasmic part [12,41] and a possible trimer of dimer oligomerization may play a crucial role for a much tighter binding. In order to obtain a system more closely related to the natural one, future studies with full length transducers [39] will most probably give more details about the complex formation.

Acknowledgements

J. F. thanks G. Büldt (Forschungszentrum Jülich) for continuous and sustainable support in his institute. This work was supported by the Deutsche Forschungsgemeinschaft (M.E.) and by a priority program SPP 1128 of Deutsche Forschungsgemeinschaft (FI 841/3-1,2 to J.F.). We are indebted to R. Schlesinger for providing us with bacteriorhodopsin and to R. Batra-Safferling for the discussions and comments on the manuscript.

Appendix A. The dependence of FRET efficiencies on protein concentration and label ratios

The calculated FRET efficiency as given in Eqs. (3) and (4) is based on the assumption that every individual donor labeled protein binds to an acceptor labeled protein. Experimentally, this requirement is not always fulfilled. The FRET efficiency depends on the total protein concentrations ($[HtrII_{total}]$ and $[SRII_{total}]$), on label ratios (f_D for the donor and f_A for the acceptor), and on which kind of dimerization (hetero or homo-dimerization) has to be considered.

Hetero-dimerization

In this kind of FRET experiment the donor labeled NpHtrII molecules $[P_D]=[HtrII_{total}]\cdot(f_D)$ can either bind to acceptor labeled NpSRII molecules $[P_A]=[SRII_{total}]\cdot(f_A)$ or to unlabeled NpSRII molecules $[P_U]=[SRII_{total}]\cdot(1-f_A)$.

$$FL=\frac{P_D\cdot P_A}{P_D\cdot P_A+P_D\cdot P_U}=f_A \tag{A1}$$

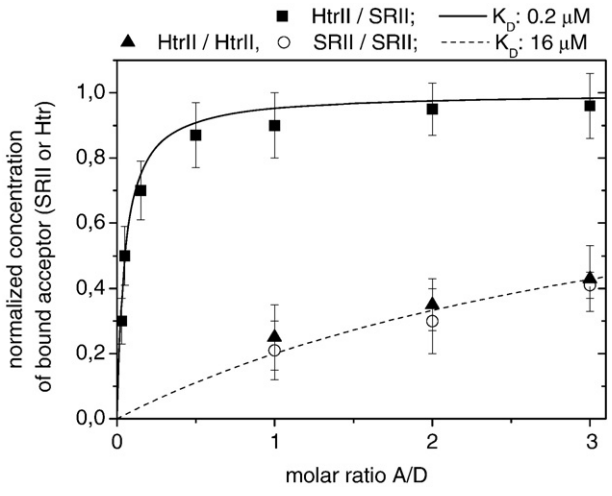

Fig. 7. FRET efficiencies measured in detergent buffer were used to calculate the fraction of bound acceptor labeled molecules as a function of the concentration of acceptor labeled molecules, the latter in terms of molar acceptor/donor ratios (Materials and methods, Eq. (5)). For the experimental data shown here donor labeled proteins at concentrations of about 4 μM were employed. For each data point 3–4 independent measurements have been performed and the error bars represent the corresponding standard deviation. Theoretical curves calculated from the corresponding dissociation constants (K_D) are shown for the hetero-dimer formation (solid line) and for homo-dimer formation (dashed line).

Homo-dimerization

In this case, FRET pairs of one and the same protein molecule (e.g., NpHtrII) are formed. Therefore, we have to consider $[P_D]=[\mathrm{NpHtrII_{D\text{-}total}}]\cdot(f_D)$, $[P_A]=[\mathrm{NpHtrII_{A\text{-}total}}]\cdot(f_A)$, and $[P_U]=[\mathrm{NpHtrII_{D\text{-}total}}]\cdot(1-f_D)]+[\mathrm{NpHtrII_{A\text{-}total}}]\cdot(1-f_A)]$. Compared to hetero-dimerization the measured FRET efficiency is further reduced by the fact that we have to consider binding pairs where both proteins are labeled with donor molecules [37].

$$FL = \frac{P_D \cdot P_A}{P_D \cdot P_A + P_D \cdot P_D + P_D \cdot P_U} \tag{A2}$$

While for hetero-dimerization the dependence on protein concentrations is canceled out, we have to consider protein concentrations for the homo-dimerization.

References

[1] J.L. Spudich, H. Luecke, Sensory rhodopsin II: functional insights from structure, Curr. Opin. Struct. Biol. 12 (2002) 540.
[2] E. Pebay-Peyroula, A. Royant, E.M. Landau, J. Navarro, Structural basis for sensory rhodopsin function, Biochim. Biophys. Acta 1565 (2002) 196.
[3] J.P. Klare, V.I. Gordeliy, J. Labahn, G. Buldt, H.J. Steinhoff, M. Engelhard, The archaeal sensory rhodopsin II/transducer complex: a model for transmembrane signal transfer, FEBS Lett. 564 (2004) 219.
[4] R. Moukhametzianov, J.P. Klare, R. Efremov, C. Baeken, A. Goppner, J. Labahn, M. Engelhard, G. Buldt, V.I. Gordeliy, Development of the signal in sensory rhodopsin and its transfer to the cognate transducer, Nature 440 (2006) 115.
[5] J.P. Klare, I. Chizhov, M. Engelhard, Microbial rhodopsins: scaffolds for ion pumps, channels, and sensors, Results Probl. Cell Differ. 45 (2008) 73.
[6] W.D. Hoff, K.H. Jung, J.L. Spudich, Molecular mechanism of photosignaling by archaeal sensory rhodopsins, Annu. Rev. Biophys. Biomol. Struct. 26 (1997) 223.
[7] J.J. Falke, G.L. Hazelbauer, Transmembrane signaling in bacterial chemoreceptors, Trends Biochem. Sci. 26 (2001) 257.
[8] H. Luecke, B. Schobert, J.K. Lanyi, E.N. Spudich, J.L. Spudich, Crystal structure of sensory rhodopsin II at 2.4 Angstroms: insights into color tuning and transducer interaction, Science 293 (2001) 1499.
[9] A. Royant, P. Nollert, K. Edman, R. Neutze, E.M. Landau, E. Pebay-Peyroula, J. Navarro, X-ray structure of sensory rhodopsin II at 2.1-A resolution, Proc. Natl. Acad. Sci. U. S. A. 98 (2001) 10131.
[10] V.I. Gordeliy, J. Labahn, R. Moukhametzianov, R. Efremov, J. Granzin, R. Schlesinger, G. Buldt, T. Savopol, A.J. Scheidig, J.P. Klare, M. Engelhard, Molecular basis of transmembrane signalling by sensory rhodopsin II-transducer complex, Nature 419 (2002) 484.
[11] A.A. Wegener, J.P. Klare, M. Engelhard, H.J. Steinhoff, Structural insights into the early steps of receptor–transducer signal transfer in archaeal phototaxis, EMBO J. 20 (2001) 5312.
[12] D.D. Oprian, Phototaxis, chemotaxis and the missing link, Trends Biochem. Sci. 28 (2003) 167.
[13] S. Hippler-Mreyen, J.P. Klare, A.A. Wegener, R. Seidel, C. Herrmann, G. Schmies, G. Nagel, E. Bamberg, M. Engelhard, Probing the sensory rhodopsin II binding domain of its cognate transducer by calorimetry and electrophysiology, J. Mol. Biol. 330 (2003) 1203.
[14] J.P. Klare, E. Bordignon, M. Doebber, J. Fitter, J. Kriegsmann, I. Chizhov, H.J. Steinhoff, M. Engelhard, Effects of solubilization on the structure and function of the sensory rhodopsin II/transducer complex, J. Mol. Biol. 356 (2006) 1207.
[15] Y. Sudo, M. Iwamoto, K. Shimono, N. Kamo, Pharaonis phoborhodopsin binds to its cognate truncated transducer even in the presence of a detergent with a 1:1 stoichiometry, Photochem. Photobiol. 74 (2001) 489.
[16] Y. Sudo, M. Iwamoto, K. Shimono, N. Kamo, Role of charged residues of pharaonis phoborhodopsin (sensory rhodopsin II) in its interaction with the transducer protein, Biochemistry 43 (2004) 13748.
[17] Y. Sudo, M. Yamabi, S. Kato, C. Hasegawa, M. Iwamoto, K. Shimono, N. Kamo, Importance of specific hydrogen bonds of archaeal rhodopsins for the binding to the transducer protein, J. Mol. Biol. 357 (2006) 1274.
[18] C.S. Yang, O. Sineshchekov, E.N. Spudich, J.L. Spudich, The cytoplasmic membrane-proximal domain of the HtrII transducer interacts with the E–F loop of photoactivated *Natronomonas pharaonis* sensory rhodopsin II, J. Biol. Chem. 279 (2004) 42970.
[19] Y. Taniguchi, T. Ikehara, N. Kamo, Y. Watanabe, H. Yamasaki, Y. Toyoshima, Application of fluorescence resonance energy transfer (FRET) to investigation of light-induced conformational changes of the phoborhodopsin/transducer complex, Photochem. Photobiol. 83 (2007) 311.
[20] Y. Taniguchi, T. Ikehara, N. Kamo, H. Yamasaki, Y. Toyoshima, Dynamics of light-induced conformational changes of the phoborhodopsin/transducer complex formed in the *n*-dodecyl beta-D-maltoside micelle, Biochemistry 46 (2007) 5349.
[21] E. Bordignon, J.P. Klare, M. Doebber, A.A. Wegener, S. Martell, M. Engelhard, H.J. Steinhoff, Structural analysis of a HAMP domain: the linker region of the phototransducer in complex with sensory rhodopsin II, J. Biol. Chem. 280 (2005) 38767.
[22] E. Li, M. You, K. Hristova, Sodium dodecyl sulfate-polyacrylamide gel electrophoresis and forster resonance energy transfer suggest weak interactions between fibroblast growth factor receptor 3 (FGFR3) transmembrane domains in the absence of extracellular domains and ligands, Biochemistry 44 (2005) 352.
[23] S.E. Mansoor, K. Palczewski, D.L. Farrens, Rhodopsin self-associates in asolectin liposomes, Proc. Natl. Acad. Sci. U. S. A. 103 (2006) 3060.
[24] A.V. Botelho, T. Huber, T.P. Sakmar, M.F. Brown, Curvature and hydrophobic forces drive oligomerization and modulate activity of rhodopsin in membranes, Biophys. J. 91 (2006) 4464.
[25] M.C. Overton, K.J. Blumer, Use of fluorescence resonance energy transfer to analyze oligomerization of G-protein-coupled receptors expressed in yeast, Methods 27 (2002) 324.
[26] J.F. Mercier, A. Salahpour, S. Angers, A. Breit, M. Bouvier, Quantitative assessment of beta 1- and beta 2-adrenergic receptor homo- and heterodimerization by bioluminescence resonance energy transfer, J. Biol. Chem. 277 (2002) 44925.
[27] V. Balannik, R.A. Lamb, L.H. Pinto, The oligomeric state of the active BM2 ion channel protein of influenza B virus, J. Biol. Chem. 283 (2008) 4895.
[28] B. Grasberger, A.P. Minton, C. DeLisi, H. Metzger, Interaction between proteins localized in membranes, Proc. Natl. Acad. Sci. U. S. A. 83 (1986) 6258.
[29] S.N. Ho, H.D. Hunt, R.M. Horton, J.K. Pullen, L.R. Pease, Site-directed mutagenesis by overlap extension using the polymerase chain reaction, Gene 77 (1989) 51.
[30] I.P. Hohenfeld, A.A. Wegener, M. Engelhard, Purification of histidine tagged bacteriorhodopsin, pharaonis halorhodopsin and pharaonis sensory rhodopsin II functionally expressed in Escherichia coli, FEBS Lett. 442 (1999) 198.
[31] J.L. Rigaud, G. Mosser, J.J. Lacapere, A. Olofsson, D. Levy, J.L. Ranck, Bio-Beads: an efficient strategy for two-dimensional crystallization of membrane proteins, J. Struct. Biol. 118 (1997) 226.
[32] V. Luzzati, Biological Membranes, Academic Press, New York, 1986.
[33] J.R. Lakowicz, Principles of Fluorescence Spectroscopy, Kluwer Academic / Plenum Press, New York, 1999.
[34] X. Michalet, S. Weiss, M. Jager, Single-molecule fluorescence studies of protein folding and conformational dynamics, Chem. Rev. 106 (2006) 1785.
[35] L.E. Fisher, D.M. Engelman, J.N. Sturgis, Detergents modulate dimerization, but not helicity, of the glycophorin A transmembrane domain, J. Mol. Biol. 293 (1999) 639.
[36] K.G. Fleming, Standardizing the free energy change of transmembrane helix–helix interactions, J. Mol. Biol. 323 (2002) 563.
[37] M. You, E. Li, W.C. Wimley, K. Hristova, Forster resonance energy transfer in liposomes: measurements of transmembrane helix dimerization in the native bilayer environment, Anal. Biochem. 340 (2005) 154.
[38] O.S. Mironova, R.G. Efremov, B. Person, J. Heberle, I.L. Budyak, G. Buldt, R. Schlesinger, Functional characterization of sensory rhodopsin II from *Halobacterium salinarum* expressed in *Escherichia coli*, FEBS Lett. 579 (2005) 3147.
[39] N. Mennes, J.P. Klare, I. Chizhov, R. Seidel, R. Schlesinger, M. Engelhard, Expression of the halobacterial transducer protein HtrII from *Natronomonas pharaonis* in *Escherichia coli*, FEBS Lett. 581 (2007) 1487.
[40] J. Otomo, W. Marwan, D. Oesterhelt, H. Desel, R. Uhl, Biosynthesis of the two halobacterial light sensors P480 and sensory rhodopsin and variation in gain of their signal transduction chains, J. Bacteriol. 171 (1989) 2155.
[41] I.L. Budyak, V. Pipich, O.S. Mironova, R. Schlesinger, G. Zaccai, J. Klein-Seetharaman, Shape and oligomerization state of the cytoplasmic domain of the phototaxis transducer II from *Natronobacterium pharaonis*, Proc. Natl. Acad. Sci. U. S. A. 103 (2006) 15428.